FREQUENCY ANALYSIS OF SHORT-PERIOD MICROSEISMS GENERATED BY TRAINS

A Thesis

Presented to the Graduate Faculty of the

New Mexico Institute of Mining and Technology

in Partial Fulfillment of the Requirements

for the Degree of Master of Science in

Geophysics.

by

Ara G. Carapetian

June, 1966

ACKNOWLEDGEMENTS

I am greatly indebted to Dr. Allan R. Sanford who supplied the train noise records and provided assistance in every step of this research work.

My special thanks go to Dr. John D. McKee for helping me to write the final manuscript of the thesis, and to Dr. Ross Lomanitz who gave very useful suggestions during my thesis work. I wish, also, to express my appreciation to Dr. Charles R. Holmes, Dr. Bhartendu and other members of the thesis committee for their help in the final preparation of this work.

Finally, I would like to thank Messrs. Ravula S. Reddy, Ramanatsoa Ramananantoadro and Surendra Singh who have helped in the computation and preparation of the data.

Financial support for this research was obtained from the Air Force Office of Scientific Research under Grant 658-64.

TABLE OF CONTENTS

LIST OF FIGURES

LIST OF TABLES

ABSTRACT

Train generated microseisms at Socorro, New Mexico, were recorded at five locations. Power spectral density analyses of the registered signals obtained by statistical methods revealed frequency peaks. At a distance of about 15000 feet from the train, frequency peaks at about 2.1 and 3.0 c/s were present. At distances of about 12000, 7000 and 2000 feet, peaks in the noise spectra were found at 3.6, 3.6, and 4.5 c/s, respectively. Two segments of a record taken at the railroad station at a distance of 6 feet from the rail-track were analyzed, one segment was noise produced by the train when it was about 6500 feet north of the station, the other when it was at about the same distance south of the station. Peaks in the noise spectrum for these examples were not the same even after correction for the Doppler shift.

For all examples of train noise, 90 percent or more of the energy was found to be concentrated in a narrow frequency range which at no time exceeded a width of 4 c/s. All of the frequency peaks established in the study lie within the 4 c/s band-width at all locations. However, the narrow band, where 90 percent of the energy is concentrated, shifts as a whole to lower frequencies with an increase in the distance between the noise source and the recording location. An increase in the distance of the recorder from the noise source also shifts the frequency peaks contained in the frequency band. However, the exact relation between distance and frequency peak shifts could not be established.

FREQUENCY ANALYSIS OF SHORT-PERIOD MICROSEISMS GENERATED BY TRAINS

INTRODUCTION

The objective of this study was to investigate the frequency spectrum characteristics of the noise generated by trains passing through Socorro, New Mexico.

In previous studies, Frantti, et al. (1962), and Walker, et al. (1964) have shown that the frequency spectrum of the microseisms contain a high-energy peak between the frequencies of 2 and 3 c/s, a peak that Walker has suggested is caused by industrial noise. In Socorro, Long (1964), on the basis of a histogram of measured frequencies, suggested two frequency peaks (at 2.9 and 3.4 c/s) in the noise produced by trains at a distance of about 15000 feet. A primary reason for the present study was to establish these peaks more accurately by determining the power spectral density of the train noise using statistical methods.

The results of the power spectral analyses indicate two peaks in the train noise at a distance of about 15000 feet, but at somewhat

different frequencies (2.1 and 3.0 c/s) than suggested by Long (1964). In addition, the analyses of this study show that 90 percent of the noise produced by trains is always restricted to a narrow frequency range (less than 4 c/s), but the band of noise shifts as a whole to higher frequencies with decrease in distance from the noise source.

THEORY

INTRODUCTION.

Two methods, one functional and the other stochastic, are used in the analysis of physical phenomena. In the functional approach, the phenomenon under investigation is assumed to be a mathematical function ideally defined for all time. Whereas, in the stochastic approach, the sample function is assumed to be randomly extracted from the universe, thus chance elements are included in the analysis. If the physical realization is limited to a single function, the stochastic approach is the same as the functional approach (Paulson, 1964, p. 11). Because the stochastic approach is more general, especially in that it includes chance elements, it was adopted for this study.

In this section some important definitions and concepts, pertinent to the development of power spectral density estimates using the stochastic approach, are presented.

DEFINITIONS.

Probability.

Probability function or probability measure: Probability function or probability measure, P(S), is defined as a real valued function which is (1) known on sets of some space, (2) non-negative, and (3) additive for unions of disjoint sets (Cramer, 1946, p. 56).

Probability distribution function: Probability distribution function, F(x), is a non-decreasing function having the following properties:

$$0 \leq F(x) \leq 1$$

$$F(-\infty) = 0 \quad \text{and} \quad F(+\infty) = 1 \ .$$

Probability density function: Probability density function, $p(x)$, is the derivative of the probability distribution function, $F(x)$, if this derivative exists (Solodovnikov, 1960, p. 65-66), i.e.,

$$p(x) = \frac{d[F(x)]}{dx} \ . \tag{1}$$

Stochastic Events.

Stochastic variable: A stochastic variable, $x_j(\omega)$, is defined over the space Ω, the probability measure, $P(S)$, of which is known. It, $x_j(\omega)$, assigns values of x for each element ω of the space Ω.

Stochastic function: Stochastic function, $x_j(t,\omega)$, is defined such that for fixed time, $t=t_o$, the stochastic function, $x_j(t_o,\omega)$, is a stochastic variable. When t is variable, $x_j(t,\omega)$, generates a set of stochastic functions known as a stochastic process. A set of stochastic functions generated by a stochastic process is an ensemble of stochastic functions (Davenport and Root, 1958, p. 39).

If ω is fixed and t is variable, $x_j(t,\omega_o)$ is said to be a physical realization, sample function, or particular history of the stochastic process (Paulson, 1964, p. 12).

Moments.

First and n^{th} moments: If x is a stochastic variable with probability density, $p(x)$, the expectation of x, $\tilde{x}$, (also first moment of x) is defined as

$$\tilde{x} = E(x) = \int_{-\infty}^{\infty} xp(x)dx, \qquad (2)$$

(Solodovnikov, 1960, p. 70). The n^{th} moment of the stochastic variable x with probability density p(x) is defined as

$$\tilde{x}^n = E(x^n) = \int_{-\infty}^{\infty} x^n p(x)dx \qquad (3)$$

(Davenport and Root, 1958, p. 49).

The first moment indicates the average, m, over the ensemble, and when the process is stationary (a concept which will be introduced later), the second moment indicates the intensity or the average power (Davenport and Root, 1958, p. 49).

Central moments: The n^{th} central moment, μ_n, of a stochastic variable x is defined as

$$\mu_n = E\left[(x-m)^n \right] = \int_{-\infty}^{\infty} (x-m)^n \, p(x)dx, \qquad (4)$$

where m is the average or the first moment. Of particular interest is the second central moment, μ_2, which is

$$\mu_2 = \sigma_x^2 = E\left[(x-m)^2 \right] = E(x^2) - \left[E(x) \right]^2 = \int_{-\infty}^{\infty} (x-m)^2 p(x)dx \qquad (5)$$

where σ_x^2 is called variance or dispersion. The positive square root of σ_x^2 is the standard deviation of the stochastic variable x (Davenport and Root, 1958, p. 49).

Joint central moments: If x_1 and x_2 are stochastic variables with

first moments m_1 and m_2, respectively, the joint central moment, μ_{11}, or covariance is defined as

$$\mu_{11} = E [(x_1-m_1) (x_2-m_2)], \quad (6)$$

where E is the mathematical expectation (Davenport and Root, 1958, p. 49-50).

THEORETICAL CONCEPTS.

Stationarity.

Stationary stochastic processes are those families of stochastic functions for which the outcome of any operation, F, averaged over the ensemble, is independent of time. In other words, the statistical properties of the process are independent of time translations across the ensemble. For example, if F is the operation to determine statistical averages over the ensemble, the process, $x_j(t)$, is stationary when

$$F \{ x_j(t_1) \} = F \{ x_j(t_2) \} \quad (7)$$

for any fixed t_1 and t_2. For non-stationary stochastic processes

$$F \{ x_j(t_1) \} \neq F \{ x_j(t_2) \} \quad (8)$$

(Bendat, 1958, p. 4).

Ergodic Hypothesis.

Assume a stationary stochastic process, $x_j(t)$. If statistical averages, $\tilde{x}$, across the ensemble are the same as the time averages, $\bar{x}$, along the time axis of any randomly chosen member of the ensemble, the process is said to be a stationary stochastic ergodic process. In other words, for such a process time and statistical averages can be

equated, i. e.,

$$\tilde{x} = \bar{x} = \lim_{T\to\infty} \frac{1}{2T} \int_{-T}^{T} [x(t)]dt \qquad (9)$$

(Solodovnikov, 1960, p. 89-90). The ergodic hypothesis has a still more practical use in time-series analysis. If a single function, which is a particular history of the stochastic process, is under investigation, it can be divided into pieces 2T long. The length 2T is chosen to be much greater than any period contained in the process. Then, the ensemble of functions, each of 2T length, represents the stochastic process. A statistical analysis of any sample randomly chosen from this ensemble is sufficient to describe the process (Bendat, 1958, p. 6-7).

The conditions for strict stationarity, which are not easily realizable, are that the ensemble averages of all the moments are independent of time. Second order stationarity, which is more easily realizable, requires only that ensemble averages of the first and second moments are independent of time. Second order ergodicity (Paulson, 1964, p. 48-49) means that first and second moments are the same across the ensemble and along any single element of the ensemble. It should be mentioned that stationarity is a necessary but not sufficient condition for ergodicity (Paulson, 1964, p. 48-49).

The ergodic hypothesis, in spite of several attempts, has not been proved (Khinchine, 1949, p. 54-55). In geophysical research, especially in time series analysis, the ergodic hypothesis has been assumed, implicitly or explicitly. In this study it was assumed that the conditions for second order stationarity and ergodicity were met,

and therefore, ensemble averages were replaced by time averages.

Autocorrelation Function.

If x_1 and x_2 are stochastic variables at times t_1 and t_2, of a real stochastic process, $x_j(t)$, the autocorrelation function, $R_x(t_1, t_2)$ is equal to the expectation of $x_1 \cdot x_2$, i. e.,

$$R_x(t_1, t_2) = E(x_1 \cdot x_2) \tag{10}$$

(Davenport and Root, 1958, p. 59). The normalized autocorrelation function, $\rho_x(t_1, t_2)$, is expressed in terms of the joint central moment, μ_{11}, and the variances, σ_1 and σ_2, of the random variables as follows:

$$\rho_x(t_1, t_2) = \frac{\mu_{11}}{\sigma_1 \sigma_2} \quad . \tag{11}$$

When the stochastic process is assumed stationary, $R_x(t_1, t_2)$ depends only upon the time lapse or lag, $\tau = t_2 - t_1$. Under this condition, the normalized autocorrelation function (11) simplifies to

$$\rho_x(\tau) = \frac{R_x(\tau) - m^2_x}{\sigma^2_x} \quad , \tag{12}$$

where $m_x = m_1 = m_2$ and $\sigma_x = \sigma_1 = \sigma_2$ (Davenport and Root, 1958, p. 59-60). If the first moment, m_x, is assumed zero, then

$$\rho_x(\tau) = \frac{R_x(\tau)}{\sigma^2_x} \tag{13}$$

Moreover, if the process is assumed ergodic, the time autocorrelation function, $C(\tau)$,

$$C(\tau) = \lim_{T\to\infty} \frac{1}{2T} \int_{-T}^{T} x(t+\tau)\, x(t)\, dt \qquad (14)$$

equals the statistical autocorrelation function, $R_x(\tau)$.

The following properties of the autocorrelation function are important:

1. The autocorrelation function for a stationary process depends upon the elapsed time difference (time lag $\tau = t_2 - t_1$) but is invariant to time translations (Bendat, 1958, p. 19-20).

2. From relation (14)

$$C(0) = \overline{x^2} \qquad (15)$$

where $\overline{x^2}$ is the average power (Solodovnikov, 1960, p. 92).

3. The autocorrelation function, $C(\tau)$, is an even function of time lag, τ, since $C(\tau) = C(-\tau)$, as shown below, assuming the process to be stationary,

$$C(\tau) = \overline{x(t)x(t+\tau)} = \overline{x(t-\tau)x(t)} = \overline{x(t)x(t-\tau)} = C(-\tau) \qquad (16)$$

(Solodovnikov, 1960, p. 92).

4. The autocorrelation function, $C(\tau)$, is bounded from above by its value at time zero (also called variance), i. e.,

$$C(0) \geq C(\tau) \qquad (17)$$

(Paulson, 1964, p. 24).

Power Spectral Density Function and Windows.

Power spectral density function: If $x(t)$ is a signal, $x_T(t)$ is defined as

$$x_T(t) = \begin{cases} x(t) & \text{when } -T \leq t \leq T \\ 0 & \text{otherwise.} \end{cases}$$

In other words, $x_T(t)$ is a truncated function of length 2T extracted from $x(t)$. The Fourier transform of the truncated function, called $X_T(j\omega)$, is

$$X_T(j\omega) = \int_{-\infty}^{\infty} x_T(t) e^{-j\omega t} dt = \int_{-T}^{T} x(t) e^{-j\omega t} dt. \tag{18}$$

The true power spectral density function, $P(\omega)$, is defined as

$$P(\omega) = \lim_{T\to\infty} \frac{1}{2T} \left| X_T(j\omega) \right|^2 \tag{19}$$

(Solodovnikov, 1960, p. 95). Also, it can be shown that

$$\overline{x^2} = \lim_{T\to\infty} \frac{1}{2\pi} \int_{-\infty}^{\infty} \frac{1}{2T} \left| X_T(j\omega) \right|^2 d\omega = \frac{1}{2\pi} \int_{-\infty}^{\infty} P(\omega) d\omega \tag{20}$$

where $\overline{x^2}$ is the average power (Solodovnikov, 1960, p. 96).

$C_T(\tau)$, the autocorrelation function for the truncated piece, $x_T(t)$ is

$$C_T(\tau) = \frac{1}{2T} \int_{-T}^{T} x_T(t) x_T(t+\tau) dt. \tag{21}$$

The true and truncated autocorrelation functions are related as

$$C(\tau) = \lim_{T\to\infty} C_T(\tau) . \tag{22}$$

Taking the Fourier transform of the auto-correlation function,

$$\int_{-\infty}^{\infty} C_T(\tau)e^{-j\omega\tau}d\tau = \frac{1}{2T}\int_{-\infty}^{\infty} e^{-j\omega\tau}d\tau \int_{-\infty}^{\infty} x_T(t)x_T(t+\tau)dt$$

$$= \frac{1}{2T}\int_{-\infty}^{\infty} d\tau \int_{-\infty}^{\infty} x_T(t)e^{j\omega t}\, x(t+\tau)e^{-j\omega(t+\tau)}dt, \qquad (23)$$

and introducing equation (18) into (23) gives

$$\int_{-\infty}^{\infty} C(\tau)e^{-j\omega\tau}d\tau = \frac{1}{2T}\left| X_T(j\omega) \right|^2. \qquad (24)$$

If we take the limit of the above expression and make use of equation (19), then

$$P(\omega) = \lim_{T\to\infty} \int_{-\infty}^{\infty} C_T(\tau)e^{-j\omega\tau}d\tau = \int_{-\infty}^{\infty} C(\tau)e^{-j\omega\tau}d\tau \qquad (25)$$

(Solodovnikov, 1960, p. 98-99). This shows that the autocorrelation function, $C(\tau)$, and power spectral density function, $P(\omega)$ (also $P(f)$), are a Fourier transform pair. Further, since the autocorrelation function is an even function, the autocorrelation function and power spectral density function are Fourier cosine transforms of each other, i. e.,

$$P(\omega) = 2\int_{0}^{\infty} C(\tau)\cos(\omega\tau)\,d\tau \qquad (26)$$

(Solodovnikov, 1960, p. 98).

Windows: It can be shown that the sample (truncated) auto-correlation function, $C_T(\tau)$ is a consistent estimate of the true auto-correlation function, that is, the following variance and probability relations hold:

$$\lim_{T\to\infty} E\{ \left| C_T(\tau) - C(\tau) \right|^2 \} = 0 \tag{27}$$

and

$$P\{ \lim_{T\to\infty} C_T(\tau) = C(\tau) \} = 1 \tag{28}$$

(Paulson, 1964, p. 51). However, for the power spectral density estimates the statements corresponding to (27) and (28) above do not hold true (Paulson, 1964, p. 52). This indicates that the truncated power spectral density function will not give a consistent estimate of the true power spectral density. One way to overcome this difficulty is by introducing spectral windows $(Q(f))$, which are bounded even functions, into the expressions, for it can be shown that for every such Q(f) the following relation holds,

$$\underset{T\to\infty}{\text{l.i.m.}} \int_{-\infty}^{\infty} Q(f)\, P_T(f)\, df = \int_{-\infty}^{\infty} Q(f)\, P(f) df. \tag{29}$$

(Paulson, 1964, p. 53). The equation (29) as applied to $Q(f)P_T(f)$ guarantees equations like (27) and (28) for power spectral density estimates (Davenport and Root, 1958, p. 63-64). In this study, spectral windows, Q(f), were used to obtain consistent estimates from the truncated data.

For every spectral window, Q(f), a corresponding lag (time) window is defined such that the Fourier transform of the one is the

other (transform pair).

Windows are chosen to possess certain properties. In addition to being bounded even functions, the principal requirements of a spectral window are that (1) the main lobe be concentrated near frequency zero, f = 0, and (2) the side lobes be as low in amplitude as possible (Blackman and Tukey, 1958, p. 14). These requirements specify that the lag window be flat and blocky, but simultaneously smooth and gently changing. Moreover, the lag window, $D(\tau)$, should vanish when $|\tau|>T_m$. Since these requirements are contradictory, several investigators have attempted compromises through trial solutions. For example, the Hamming lag window, $D(\tau)$, is given as

$$D(\tau) = \begin{cases} 0.54 + 0.46 \cos\left(\frac{\pi\tau}{T_m}\right) & \text{when } |\tau|<T_m \\ 0 & \text{otherwise} \end{cases} \tag{30}$$

where $|\tau| = (t_2-t_1)$, is the time lag and T_m is the maximum lag (Blackman and Tukey, 1958, p. 98). The Hamming spectral window, $Q(f)$, which results from taking the Fourier transformation of the lag window, is given by

$$Q(f) = 0.54Q_0(f) + 0.23\,[Q_0(f + 1/2\ T_m) + Q_0(f - 1/2\ T_m)] \tag{31}$$

where

$$Q_0(f) = \frac{\sin(2\pi f T_m)}{\pi f} \tag{32}$$

(Blackman and Tukey, 1958, p. 95-98). Hamming windows were used exclusively in this study (Fig. 1).

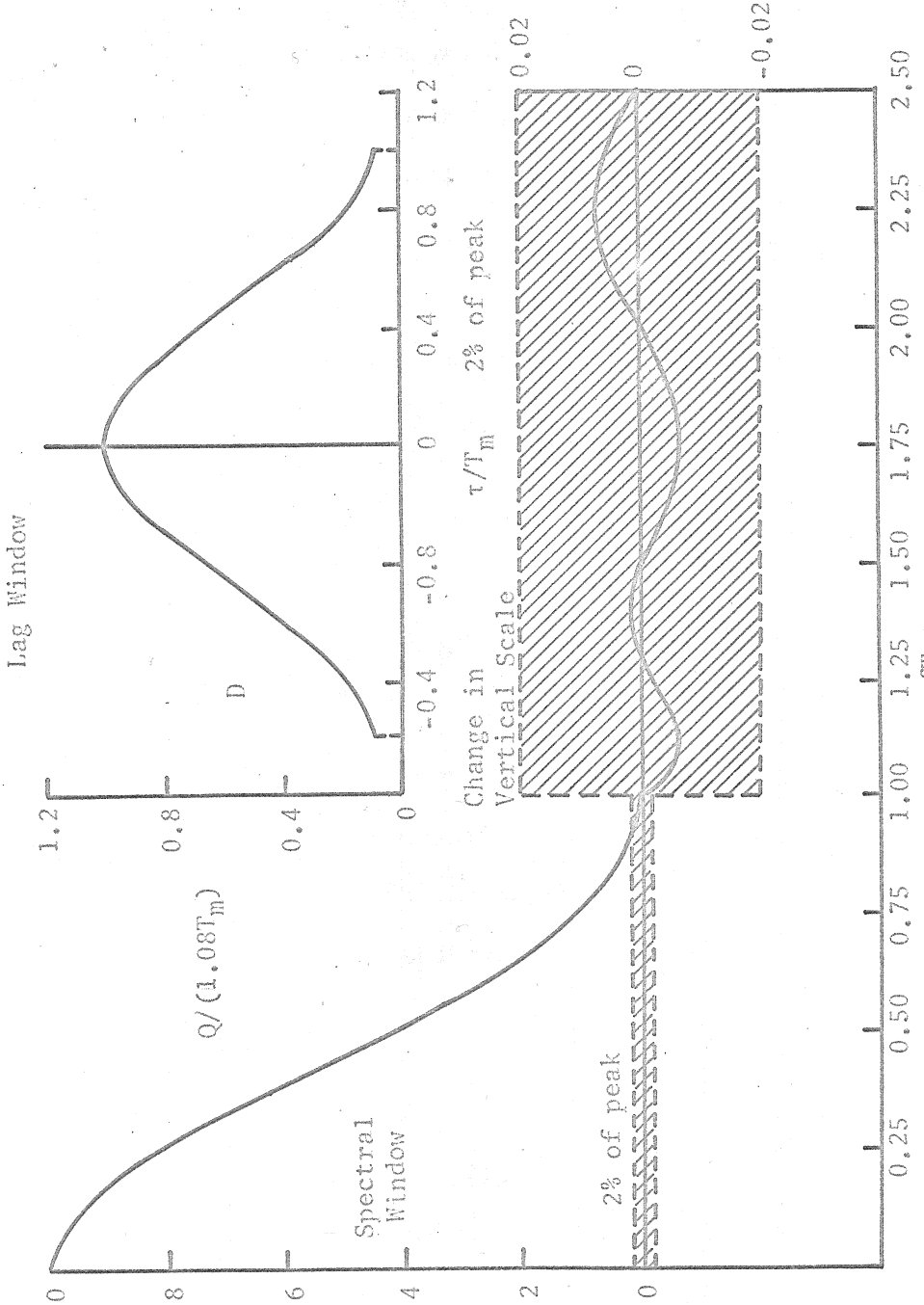

Figure 1. Hamming lag and spectral windows (from Blackman and Tukey, 1958, p. 15).

METHOD APPLIED

In the previous section, the basic theory of the power spectral density estimation for continuous data was introduced. The autocorrelation function and power spectral density estimates were derived under assumptions of second order stationarity and ergodicity.

When the data are in discrete form, the above formulas can be modified without any additional assumptions. Equations for the case of discrete data and a discussion of the confidence limits on power spectral density estimates are presented below.

DISCRETE DATA.

Aliasing.

Aliasing of frequencies is introduced when the signal is digitized at equi-spaced intervals. Thus in this study, aliasing can be considered the contribution of power in the higher frequencies to the power in the lower frequencies, which, if not considered, may lead to spurious results (Bendat, 1958, p. 52).

Suppose that the truncated function, $X_T(t)$, is digitized at intervals, Δt,

$$0,\ \Delta t,\ 2\Delta t,\ \ldots\ ,\ (n-1)\Delta t,\ T_n\ .$$

The power spectral estimate, $P_A(f)$, calculated from such digitized data, covers only the frequencies, $0 \leq f \leq f_N$, where

$$f_N = \frac{1}{2\Delta t}\ . \tag{33}$$

In this instance, f_N is said to be the Nyquist or folding frequency.

The power spectral estimate, $P_A(f)$, vanishes at frequencies higher than f_N, i. e.,

$$P_A(f) = \begin{cases} P_a(f) & \text{when} \quad 0 \leq f \leq f_N \\ 0 & \text{otherwise,} \end{cases}$$

where $P_a(f)$ is the aliased power spectrum.

If the highest frequency in the signal falls within the interval $0 \leq f \leq f_N$, the power spectral estimates derived from digitized signal at intervals $\Delta t = 1/2f$ will not be aliased (Shannon, 1949, p. 11) and as a result,

$$P_A(f) = P_a(f) = P(f), \tag{34}$$

where $P(f)$ is the true power spectral density estimate. However, if frequencies higher than $f = f_N$ exist in the original signal, they will contribute some power to the lower frequencies. The contribution of aliasing in any frequency range

$$0 \leq f \leq f_N,$$

comes from the frequencies

$$2nf_N \pm f,$$

where n is an integer, n = 1, 2, 3, ..., n (Blackman and Tukey, 1958, p. 32, p. 120).

Numerical Estimation.

The formulas for the numerical estimation of the autocorrelation function and power spectral density for discrete data are given below.

The autocorrelation function with the lag interval $\Delta\tau = h\Delta t$ is

$$C_r = \frac{1}{n-rh} \sum_{q=0}^{q=n-hr} X_q \, X_{q-hr} \,, \tag{35}$$

where, $r = 0, 1, 2, \ldots, m$, $m \leq \frac{n}{h}$. The constant h, in most practical cases is chosen equal to one (Blackman and Tukey, 1958, p. 120).

The raw spectral density estimate is

$$V_r = \Delta\tau[C_0 + 2 \sum_{q=1}^{q=m-1} C_q \cos\left(\frac{qr\pi}{m}\right) + C_m \cos(r\pi)], \tag{36}$$

where frequencies corresponding to r are $r/2m\Delta\tau$ (Blackman and Tukey, 1958, p. 121).

At this stage, the window is introduced to smooth the raw spectral estimates. The convolution integral in the continuous case simplifies to a summation process for the discrete data. In this investigation the Hamming window was used to smooth the raw power spectral estimates. The Hamming window provides a three-point smoothing with weights of 0.23, 0.54, 0.23. As a result, refined or smoothed spectral estimates, U_r, are

$$U_r = 0.23V_{r-1} + 0.54V_r + 0.23V_{r+1}, \tag{37}$$

where $1 \leq r \leq m-1$ (Blackman and Tukey, 1958, p. 36).

CONFIDENCE LIMITS OF THE ESTIMATES.

The reliability of power spectral density estimates could be tested accurately if the processes under investigation were Gaussian. The processes under investigation are not necessarily Gaussian. However, by assuming an approximate Gaussian process, some tests of the accuracy of the estimates have been devised (Blackman and Tukey, 1958, p. 15-25).

These tests were used in the study, although the approximate Gaussian character of the processes was not established.

In all, there are two variables in the power spectral density estimation, the effective length of the record, T'_n (in this study $T'_n = T_n$), and the maximum lag, T_m. The stability of estimates is directly proportional to the ratio T'_n/T_m (Blackman and Tukey, 1958, p. 112). For practical considerations, it is suggested that for any estimation the inverse of this ratio should not exceed 0.1, i. e., $T_m/T'_n \leq 0.1$ (Blackman and Tukey, 1958, p. 11). This means that if the power spectral density estimate is smooth, the root mean square (RMS) deviation of any estimate is below one-third of its average value (Blackman and Tukey, 1958, p. 21). In all the cases of this study, this ratio, T_m/T'_n, was kept within the limits suggested above.

The safest measure of stability is the similarity of results when a computation is repeated several times (Blackman and Tukey, 1958, p.21). If the results of power spectral computations are nearly the same for phenomena under relatively similar conditions, the estimate has a high degree of stability.

ANALYSIS OF THE DATA

SEISMOMETER LOCATIONS.

Microseisms, generated by trains passing through Socorro, have been recorded at the five locations shown in Figure 2. These locations were as follows:

Location No. 1 (West): Seismometers were located 7440 feet west of the New Mexico Institute of Mining and Technology (NMIMT) campus.

Location No. 2 (Vans): The seismometer was located 4625 feet west of the NMIMT campus.

Location No. 3 (R&DD): The seismometer was located in a small basement room adjacent to the elevator in the Research and Development Division Building on the NMIMT campus.

Location No. 4 (Latham's): The seismometer was located at a farm house northeast of Socorro.

Location No. 5 (Station): The seismometer was located at a distance of six feet from the track at the Santa Fe depot.

At Location No. 1, three seismometers were oriented to register vertical, north-south, and east-west components of the velocity of the ground motion, whereas, at Locations 2 through 5 only the vertical component of the ground velocity was recorded.

Table 1 is a list of the seismometer locations with their respective elevations and distances from the railroad track.

INSTRUMENTATION.

Willmore seismometers were used as ground motion detectors at all stations. Mechanically these units behave as displacement meters

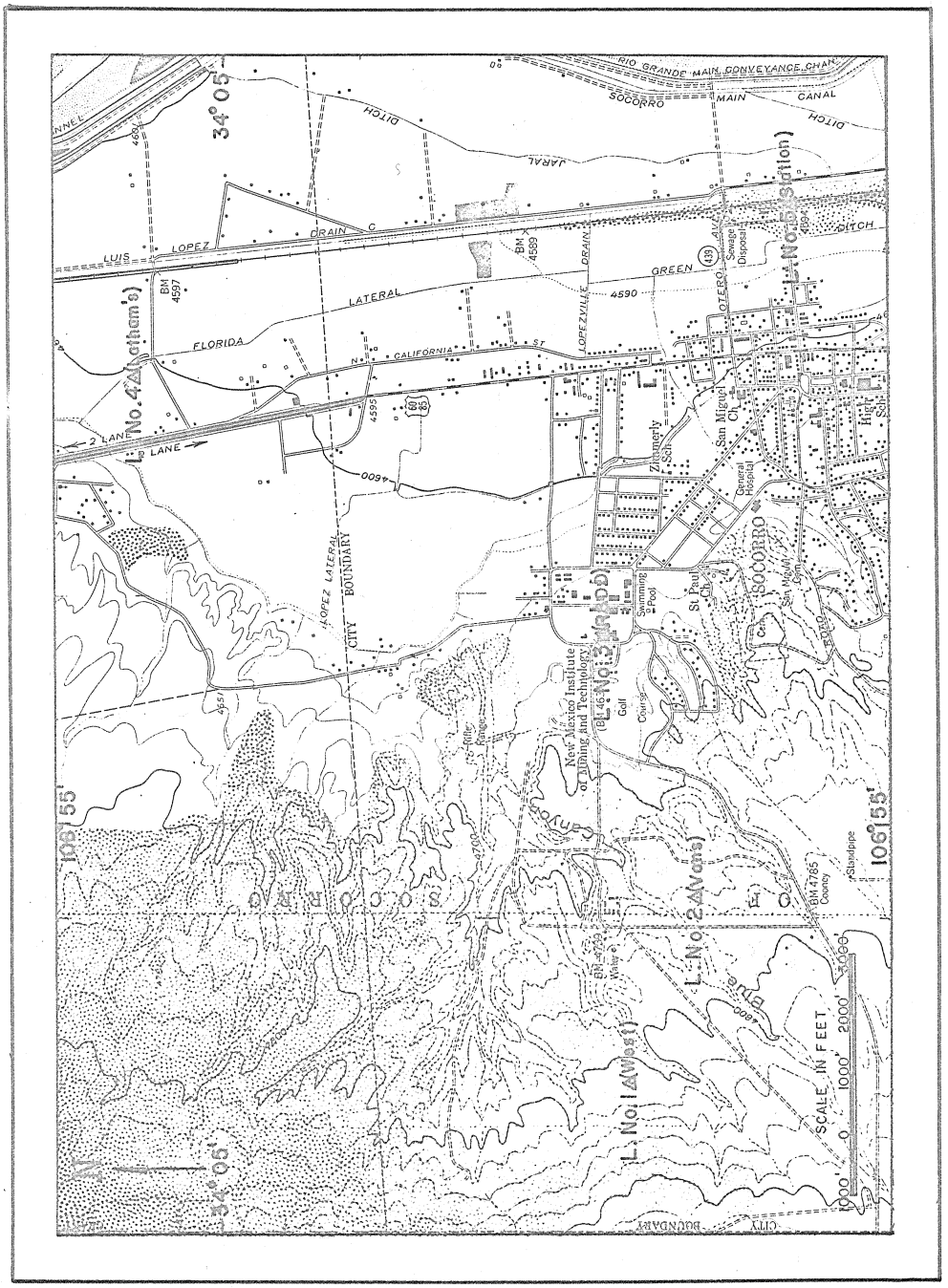

Figure 2. Map showing the Socorro area and the seismometer locations.

Table 1. Elevation and Distances of Seismometer Locations.

Location No.	Elevation in Ft.	Distance from Rail Track
1	4810	14125
2	4770	11250
3	4639	6750
4	4600	1750
5	4590	6

for frequencies above their natural frequency (1.43 c/s was the approximate natural frequency during this study). However, because the signal from the seismometer is generated by relative motions between a coil and a permanent magnet, the output is proportional to ground velocity (the open circuit response is about 1 volt per unit ground velocity of 1 cm./sec.).

The frequency response of the recording system (excluding the seismometer) at Location No. 1 was flat from 2 to 5 c/s (Long, 1964, p. 9). The frequency response curve drops rapidly after 5 c/s. At Locations 2 through 5 the response of the recording units was flat from zero c/s to at least 50 c/s.

The signal registered by the recorders at the five locations represents the velocity of the ground motion, consequently power spectral density functions (also, power spectra) computed from these signals are the power spectral estimates of the velocity of the ground motion generated by trains.

ANALYSIS OF THE RECORDS.

The response of the recording units and the components of ground motion recorded at the five locations suggests the data can be grouped as follows:

1. The records taken at Location No. 1.
2. The records taken at Locations 2 through 5.

The records taken at Location No. 1, understandably, did not contain frequency components higher than 5 c/s since the frequency response of the recording unit drops sharply beyond that frequency. For this reason, a folding frequency (Nyquist), f_N, of 7-1/2 c/s was

selected for the analysis of the records taken at this location. In this case, the digitization time interval, Δt, was $\Delta t = 1/2f_N = 1/15$ second.

No appreciable amount of high frequency noise was present in the records taken at Locations 2, 4 and 5. As for the record taken at Location No. 3, it did contain high frequency noise which was removed manually before digitization. It should be pointed out that the high-frequency noise at Location No. 3 was not generated by the train.

The details of the digitization process, folding frequency, f_N, time interval Δt, frequency resolution Δf, etc., are presented in Table 2.

THE COMPUTER PROGRAM.

A computer program (Appendix) was obtained from Bhartendu (Ph.D. Thesis, 1964). The input data for this program were the amplitude readings, X_i, at intervals Δt from the train records. The program performs the following steps:

1. Computes the mean value of X_i (input data), $\overline{X}$,

$$\overline{X} = \frac{1}{n+1} \sum_{i=0}^{n} X_i \tag{38}$$

where n+1 is the number of the data points,

2. computes the deviation from the mean, X'_i,

$$X'_i = X_i - \overline{X}, \tag{39}$$

which guarantees a zero mean for the data X'_i,

3. computes the autocorrelation function, C_r,

$$C_r = \frac{1}{n-r} \sum_{q=0}^{n-r} X'_q \, X_{q+r} \tag{40}$$

Table 2. Details of Digitization for the Records Analyzed.

Loc. No.	Date	Recording Speed	Pieces Analyzed	T_n for Ea. Piece	Δt and f_N	Max. Lag T_m, No. Solutions	Freq. Resolution Δf	High Freq. Noise Level
1	3/6/64	30 mm/sec	Nine	33.4 sec	1/15 sec 7.5 c/s	3.34 sec 51 sol.	0.15 c/s	Negligible
2	-	125/6 "	One	50 sec	6/125 sec 10.4 c/s	2.5 sec 53 sol.	0.2 c/s	Negligible
3	3/27/65	125/6 "	One	50 sec	9/125 sec 7.0 c/s	2.5 sec 36 sol.	0.2 c/s	Smoothed Manually
4	8/20/65	125 "	One	50 sec	1/25 sec 12.5 c/s	2 sec 51 sol.	0.25 c/s	Negligible
5	8/24/65	125 "	Two	30 sec	1/25 sec 12.5 c/s	2 sec 51 sol.	0.25 c/s	Negligible

where, r=0, 1, 2, ..., m, and m+1 is the number of solutions,

4. computes the raw power spectra, V_r,

$$V_r = C_0 + 2 \sum_{q=1}^{m-1} C_q \cos\left(\frac{qr\pi}{m}\right) + C_m \cos(r\pi) \tag{41}$$

where r=0, 1, 2, ..., m, and

5. finally, computes the smoothed power spectra, U_r,

$$U_r = \gamma V_{r-1} + \beta V_r + \delta V_{r+1} \tag{42}$$

where γ, β and δ are in the Hamming window weights (0.23, 0.54, 0.23, respectively). U_0 and U_m are computed as

$$U_0 = 0.54V_0 + 0.46V_1 \tag{43}$$

$$U_m = 0.46V_{m-1} + 0.54V_m \ . \tag{44}$$

In steps (1) and (3),

$$n\Delta t = T_n \tag{45}$$

$$m\Delta t = T_m \tag{46}$$

where T_n is the total time of the record digitized and T_m is the maximum lag.

RESULTS

The recorded signals, which indicate the velocity of the ground motion generated by the trains, were digitized manually at the intervals specified in Table 2 and this data fed into a computer (IBM 1620, models I and II). The results of these computations (the smoothed power spectra, and the normalized autocorrelation functions) are presented in this section. In Figures 4, 5 and 6, the results from the three-component records taken at Location No. 1 are presented, and in Figures 7, 8 and 9, the results from the records taken at Locations 2, 3 and 4 are given. Two separate segments of the record taken at Location No. 5 were digitized, each segment being the noise produced by the train when its position with respect to the seismometer was as shown in Figure 3 (below).

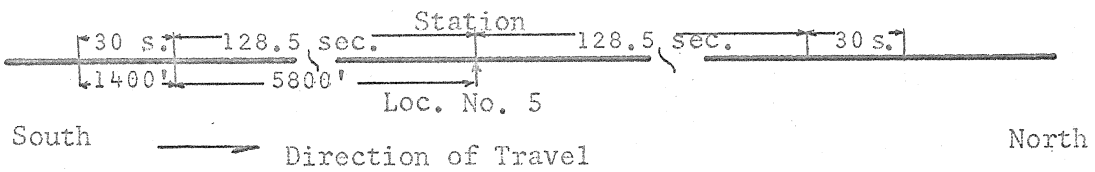

Figure 3. The position of the train with respect to the recording Location No. 5.

Figures 4, 5 and 6 are power spectra from a Location No. 1 record of a south bound train. Figure 4 shows the power spectra when the train is north of Socorro, Figure 5 when the train is at the station, and Figure 6 when the train is south of Socorro. All three components of the noise are analyzed.

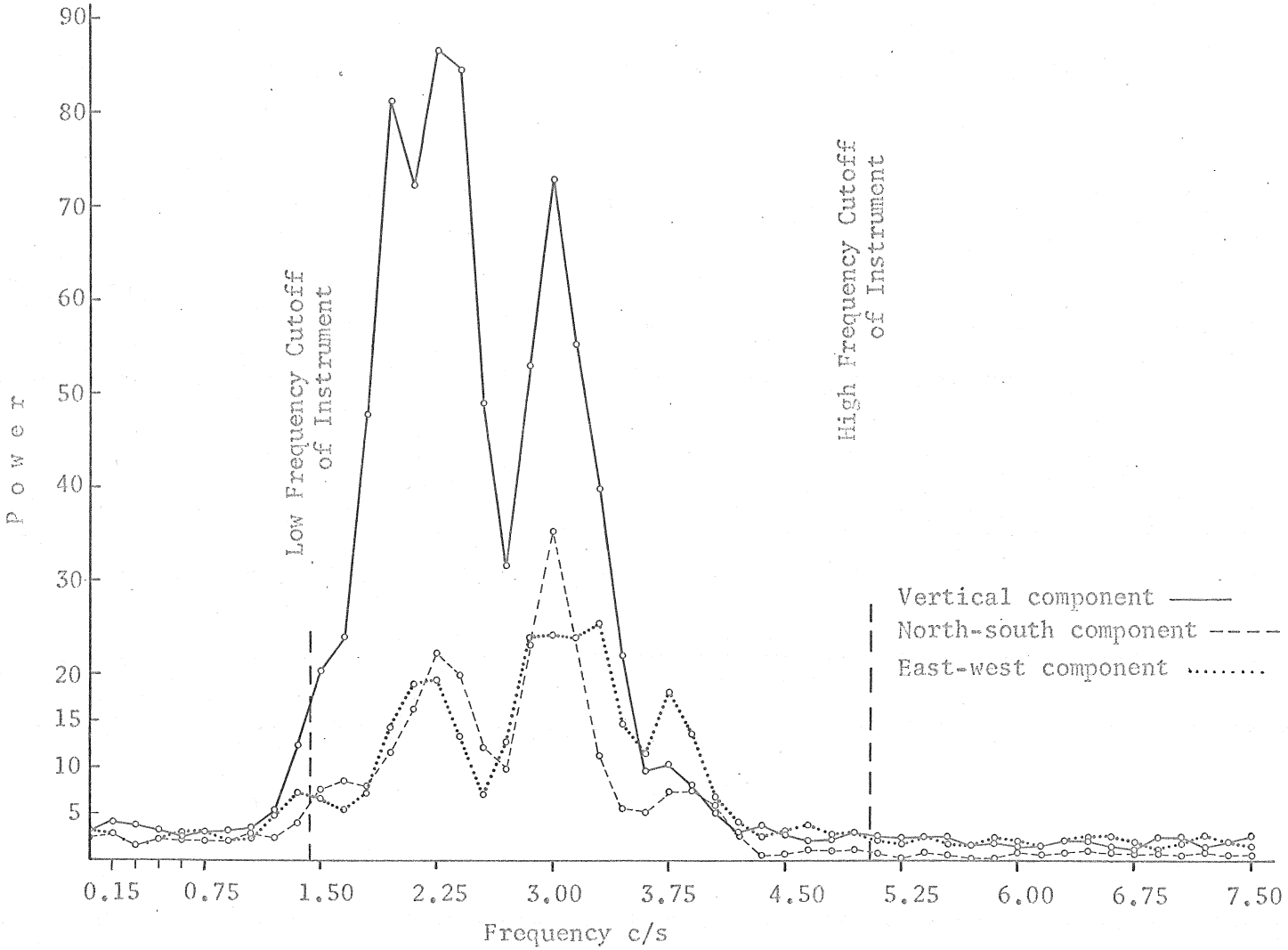

Figure 4. Power spectral density of the train noise recorded at Location No. 1 when train was north of Socorro.

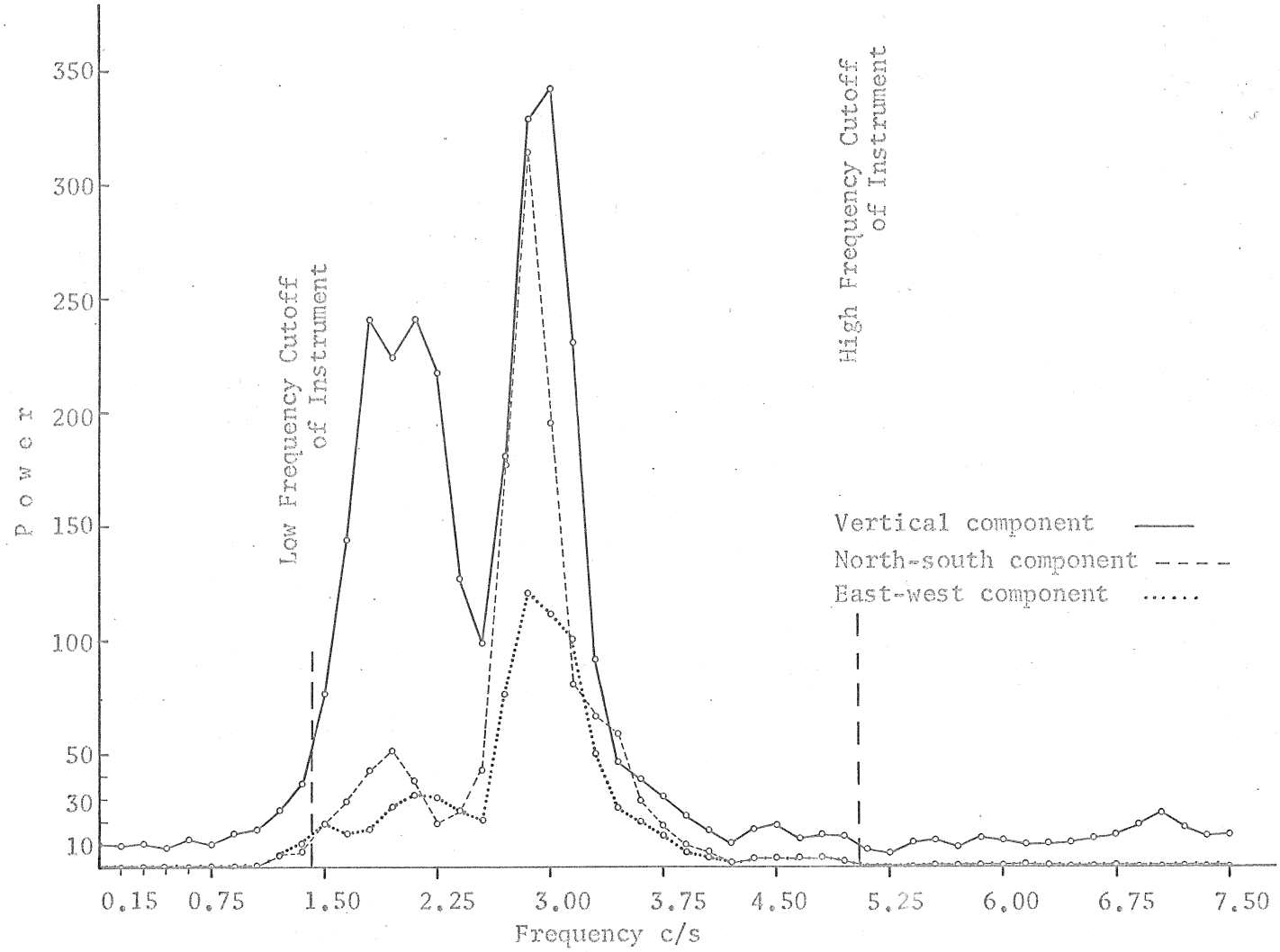

Figure 5. Power spectral density of the train noise recorded at Location No. 1 when train was approximately at the railroad station.

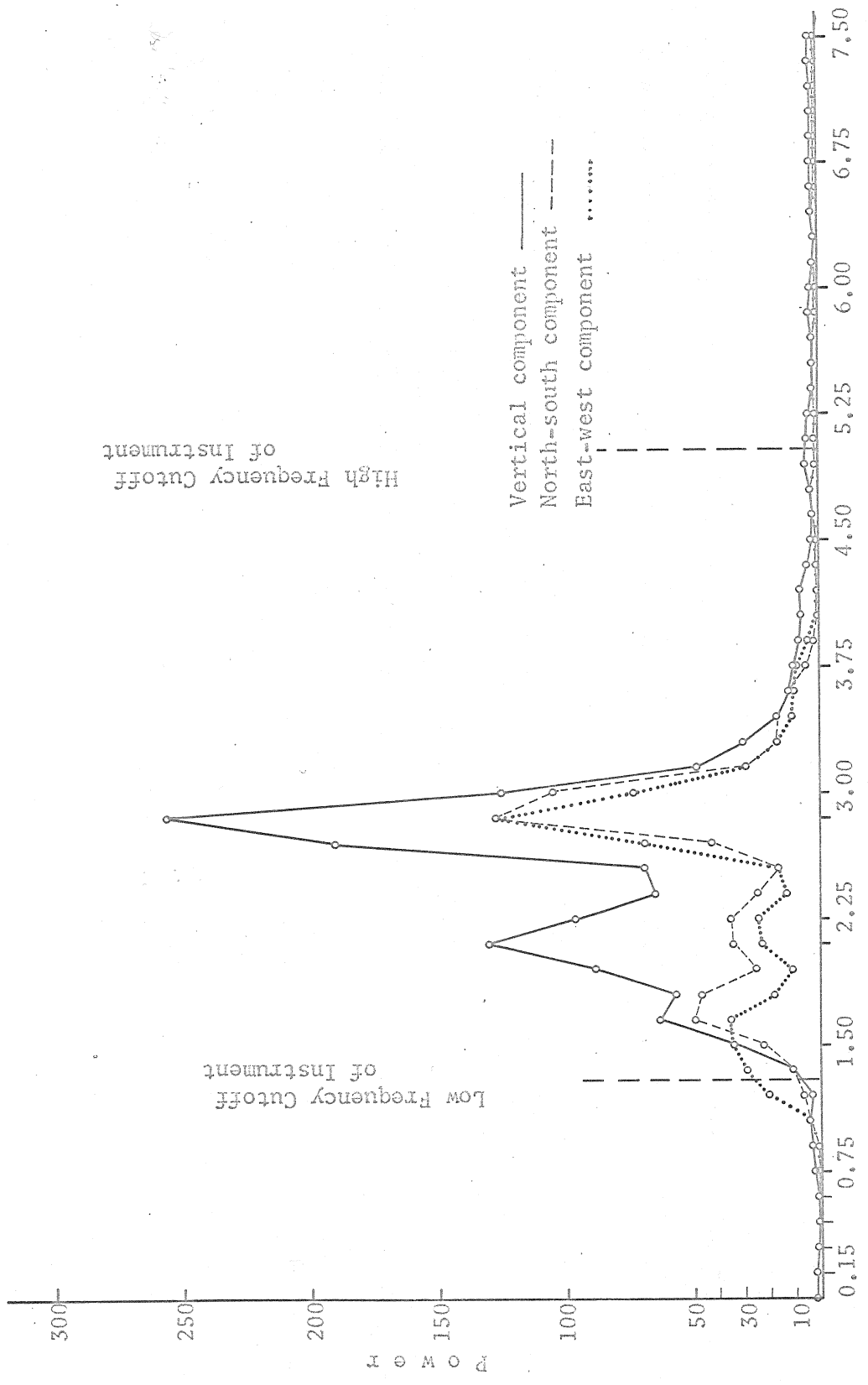

Figure 6. Power spectral density of the train noise recorded at Location No. 1 when train was south of Socorro.

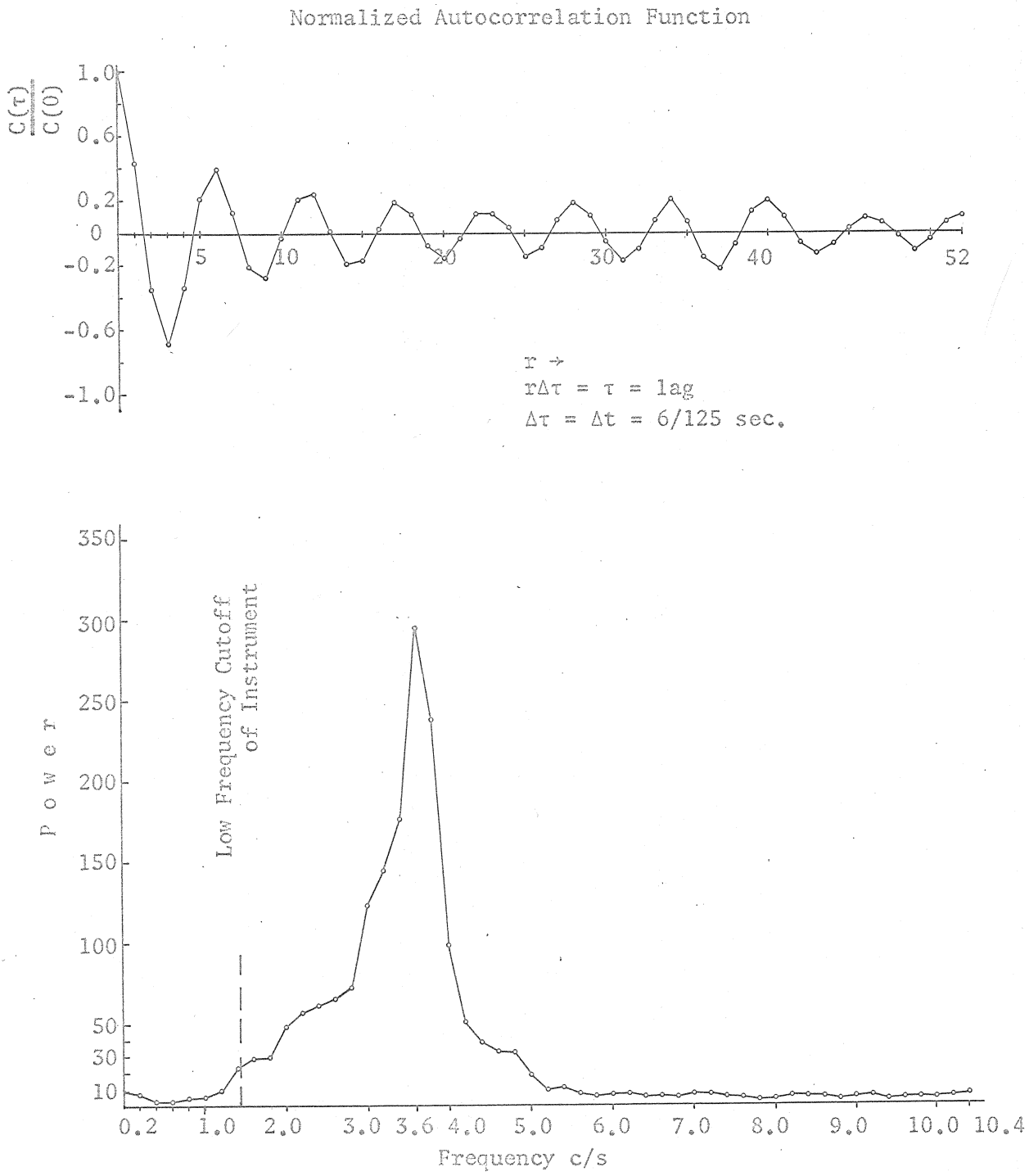

Figure 7. Power spectral density and normalized autocorrelation function (top of figure) of the train noise recorded at Location No. 2.

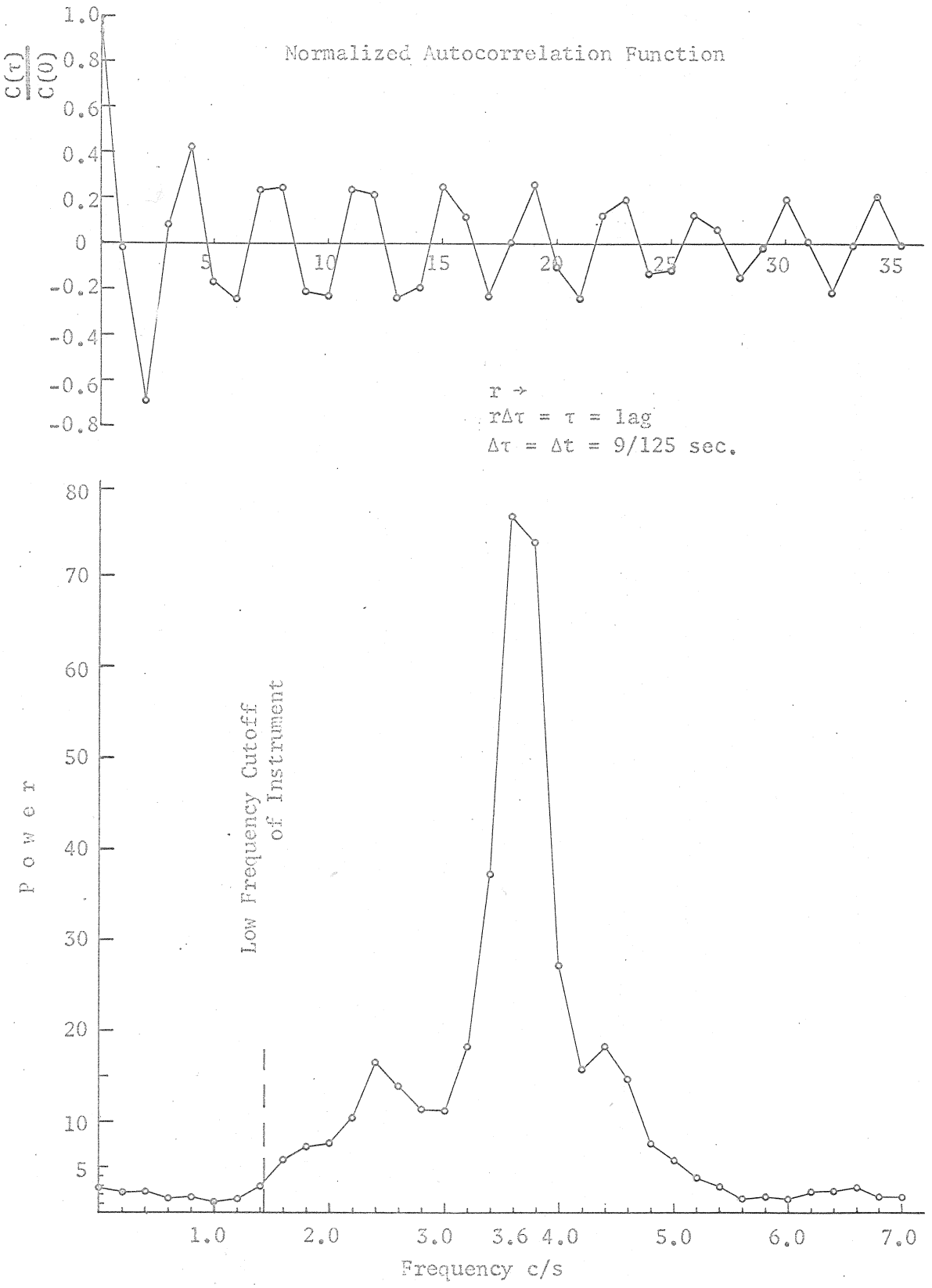

Figure 8. Power spectral density and normalized autocorrelation function (top of figure) of the train noise recorded at Location No. 3.

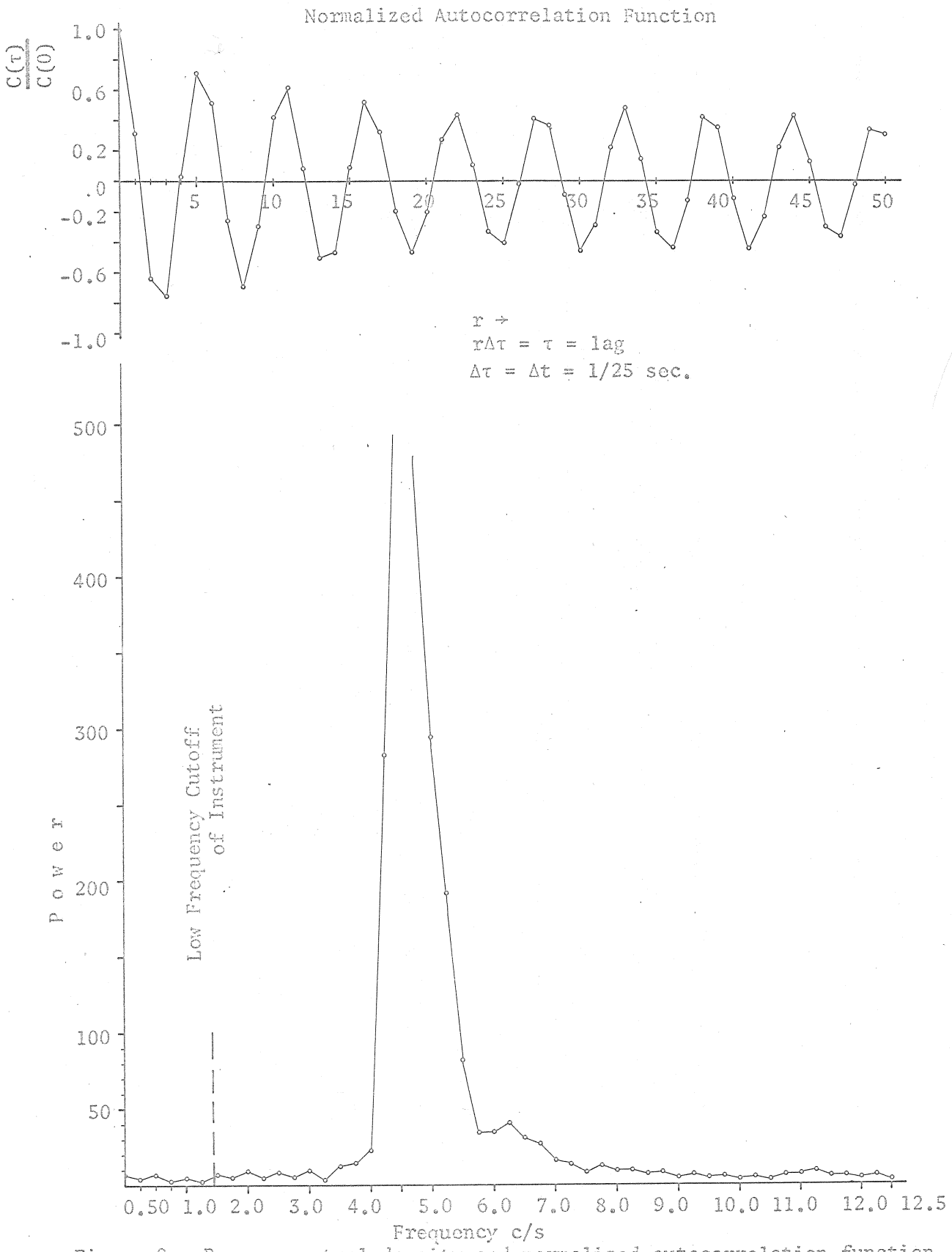

Figure 9. Power spectral density and normalized autocorrelation function (top of figure) of the train noise recorded at Location No. 4.

The graphs in Figures 4, 5 and 6 show two distinct noise peaks: one at about 3.0 c/s, the other at about 2.1 c/s. The peak at 3.0 c/s appears to be sharper and more prominent than the peak at about 2.1 c/s. In general, the results of the power spectra estimates taken from the records at Location No. 1 are quite similar. This indicates a high degree of stability in the estimates (Blackman and Tukey, 1958, p. 21).

The power spectral density estimates from the records taken at seismometer Locations 2, 3 and 4 (Figs. 7, 8 and 9) each show a distinct peak at frequencies of 3.6, 3.6 and 4.5 c/s, respectively. For these three estimates, the normalized autocorrelation functions are also plotted (top of Figs. 7, 8 and 9). The normalized autocorrelation functions in all these cases show average frequencies corresponding to the frequency peaks in the power spectra estimate plots.

The plots of power spectra estimates from the record taken at Location No. 5 are shown in Figures 10 and 11. Figure 10 shows two peaks at frequencies of 3.0 and 4.0 c/s, while in Figure 11 the peaks are at 3.5 and 4.75 c/s. The difference in frequency peaks is unexpected since the positions of the train for these examples were symmetric with respect to the seismometer at Location No. 5 (Fig. 3).

By applying a correction to remove the Doppler effect (Sears and Zemansky, 1955, p. 395), the peaks in Figure 10 are changed to 3.1 and 4.13 c/s, and the peaks in Figure 11 are changed to 3.4 and 4.6 c/s. The Doppler effect was calculated using a train velocity of 31 mph and a Rayleigh wave velocity of 1350 feet per second (Long, 1964, p. 34). The corrections made for the Doppler effect are not significant since the magnitude of the correction is less than the frequency resolution, 0.25 c/s, of the estimation.

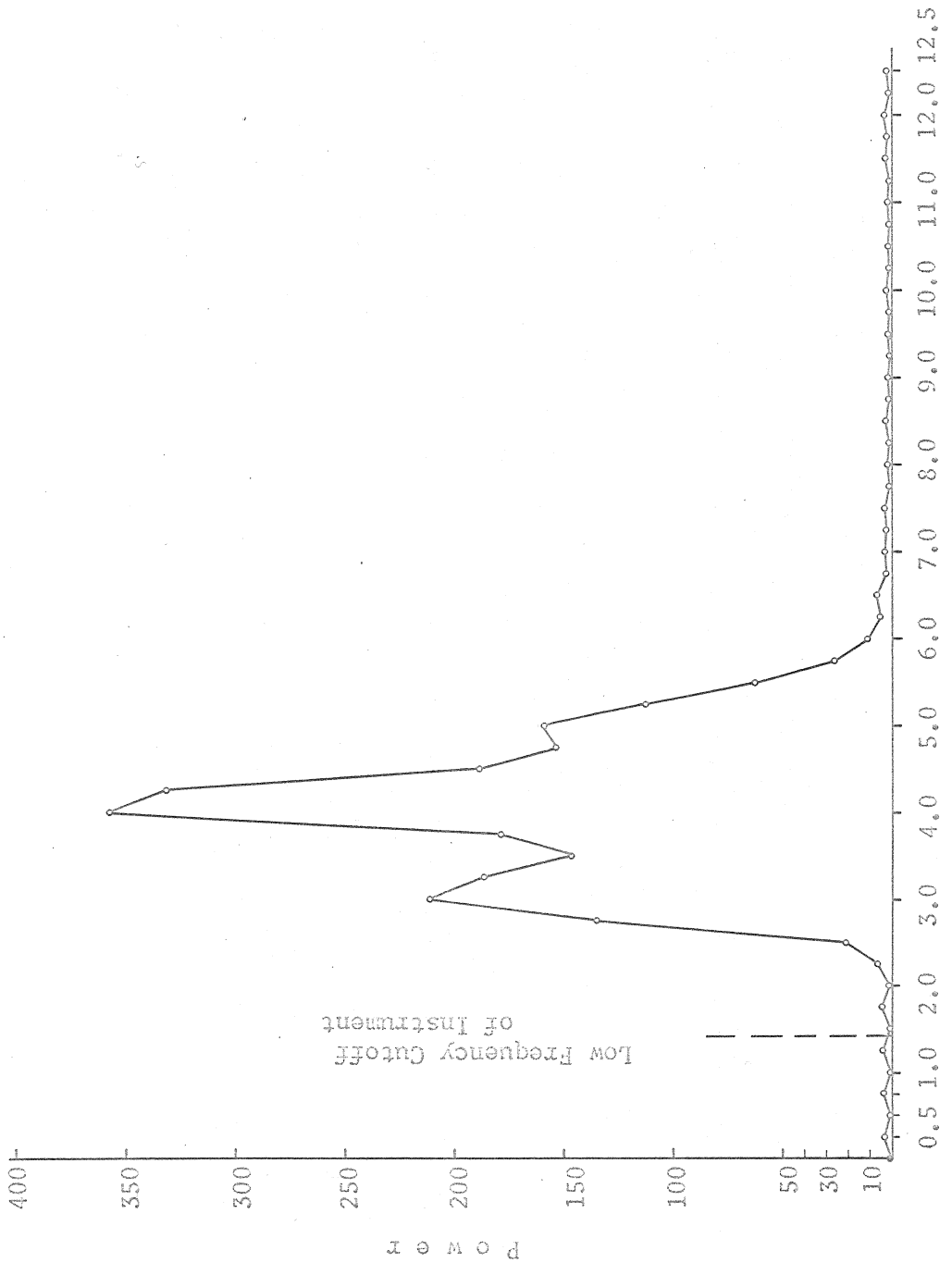

Figure 10. Power spectral density of the train noise recorded at Location No. 5 when train was north of the railroad station.

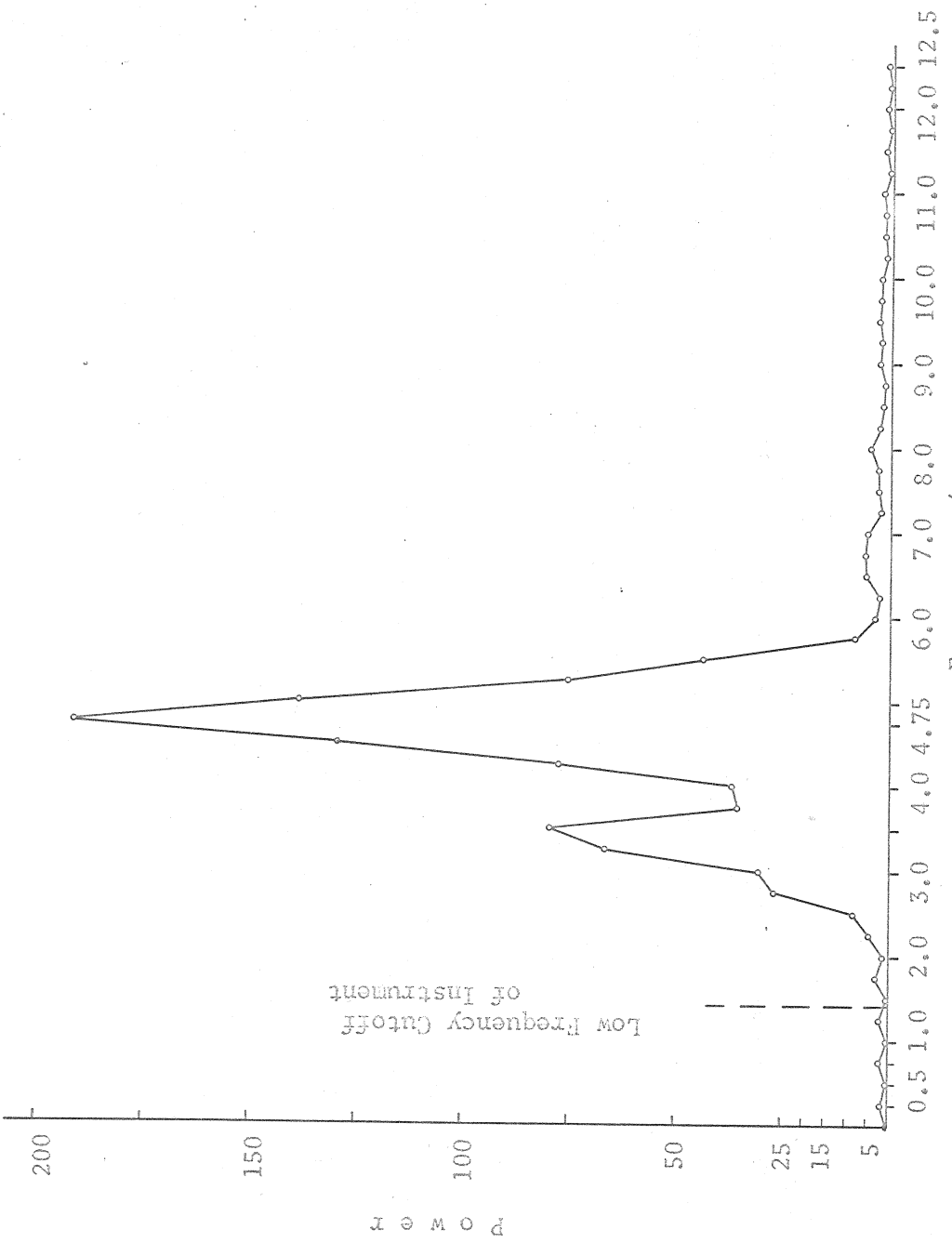

Figure 11. Power spectral density of train noise recorded at Location No. 5 when train was south of the railroad station.

In explaining the difference in frequency peaks, it should be mentioned that when the train is south of the seismometer Location No. 5, it is in a narrow part of the valley where the terrain is rugged. In contrast, when the train is north of the seismometer Location No. 5, it is in a wider part of the valley where there is almost no topographic relief.

In Table 3 all significant frequency peaks for the analyzed records are tabulated. These peaks were tested according to the arguments put forward by Blackman and Tukey (1958, p. 15-25) and found to be significant.

In all of the records used in this study, high-frequency components (higher than 5 c/s) were absent or negligible. This means that there is no significant amount of energy contribution from high frequencies (aliasing) in the power spectra estimates.

Table 3. Predominant Frequency Peaks in the Power Spectra Estimates of the Train Generated Noise.

Seis. Loc. No.	Date Record Taken	Predominant Peaks in c/s						Plotted in Figure	Train* Location	Approx. Dist. from Seismometer
		Vertical Comp.		North-South Comp.		East-West Comp.				
1	3/6/64	1.95-2.25	3.00	2.25	3.00	2.25	2.85-3.30	4	N. of Socorro	17000
1	3/6/64	1.80-2.10	3.00	1.95	2.85	-	2.85	5	At Station	14000
1	3/6/64	2.10	2.85	1.65-2.25	2.85	1.65-2.25	2.85	6	S. of Socorro	17000
2	-	-	3.60	-	-	-	-	7	At Station	12000
3	3/27/65	-	3.60	-	-	-	-	8	At Station	7000
4	8/20/65	-	4.50	-	-	-	-	9	N. of Socorro	2000
5	8/24/65	3.00	4.00	-	-	-	-	10	N. of Socorro	6500
5	8/24/65	3.50	4.75	-	-	-	-	11	S. of Socorro	6500

* Determined from amplitude of microseisms which are greatest when the train is at or near the minimum distance from the detector.

CONCLUSIONS AND SUGGESTIONS FOR FURTHER STUDY

The conclusions from the frequency analyses of the train-generated noise in Socorro can be summed up as follows:

1. At Location No. 1 two predominant frequency peaks in the plots of power spectra are present, one at about 2.1 c/s and the other at 3.0 c/s.

2. At all locations, 90 percent or more of the energy is contained in a narrow frequency range which does not exceed 4 c/s. All frequency peaks are found to lie within the 4 c/s bandwidth at all locations.

3. The narrow band, where 90 percent or more of the energy is concentrated, shifts as a whole to lower frequencies with an increase in the distance between the noise source and the recording system.

4. The distance of the recorder from the noise source also appears to be an important factor in the location of frequency peaks in the power spectra plots. The frequency peaks shift to lower frequencies with increase in the distance between the noise source and the recording system. However, the relation between distance and shift in frequency peaks does not appear to be linear.

Further experiments should be performed to check and clarify the relations between distance from the noise source and the frequency peaks in power spectra. For this purpose, it is feasible to use any seismometer with a natural period of one second or more and a recording system having a flat response for a wide frequency range. Measurements of noise should be made in an area where the topographic relief is a minimum. It would also be advantageous if the seismometers

could be equally spaced in a straight line perpendicular to the rail-track. After relations between distance and frequency are established, some analyses of the effect of rugged terrain might be of interest.

APPENDIX

Computer Program of Power Spectral Density Estimation in Fortran Language

```
      DIMENSION X(2000), SOL(500)
  100 SUMX=0.0
      READ 301
  301 FORMAT(55H
      TYPE 301
      PUNCH 301
      READ 1,ALPHA,BETA,GAMMA,DELTA,EPS,ZETA,C,NN,NR,NS
    1 FORMAT(7F7.4,3I4)
      READ 2,(X(I),I=1,NN)
    2 FORMAT(16F5.1)
      DO 3 I=1,NN
    3 SUMX=SUMX+X(I)
      ANN=NN
      XBAR=SUMX/ANN
   99 FORMAT(15X,4HSUMX,15X,4HXBAR)
    4 FORMAT(8X,F11.3,12X,F7.3)
      SUMX=0.0
      DO 5 I=1,NN
    5 X(I)=X(I)-XBAR
   77 FORMAT(//19X,12HX*=X(I)-XBAR)
   78 FORMAT(5(2X,F14.7))
  204 J2=NR+1
      DO 8 I=1,J2
      J3=NN-I
      DO 9 J=1,J3
      K=J+I-1
    9 SUMX=SUMX+X(J)*X(K)
      DEN=NN-I
      SOL(I)=SUMX/DEN
      IF(SENSE SWITCH 2) 206,8
  206 TYPE 207,I
  207 FORMAT(2HC(,I3,13H ) CALCULATED)
    8 SUMX=0.0
   81 PUNCH 83
      TYPE 83
   83 FORMAT(//19X,14HAUTOCOVARIANCE)
      PUNCH 84,(SOL(I),I=1,J2)
      TYPE 84, (SOL(I),I=1,J2)
   84 FORMAT(5(2X,F14.7))
      X1=SOL(1)
      ANR=NR
      J1=NS+1
      DO 50 I=1,J1
      J2=NR-1
      AK1=I-1
      SUM=0.0
      DO 51 J=1,J
```

```
      AJ=J
   51 SUM=SUM+SOL(J+1)*COSF(AK1*AJ*3.1416/ANR)
   50 X(I)=X1+2.*SUM+SOL(NR+1)*COSF(AK1*3.1416)
      PUNCH 85
      TYPE 85
   85 FORMAT(//19X,14HPOWER SPECTRUM)
      PUNCH 86,(X(I),I=1,J1)
      TYPE 86, (X(I),I=1,J1)
   86 FORMAT(5(2X,F14.7))
      DO 500 I=1,J1
  500 SOL(I)=0.0
      SOL(1)=BETA*X(1)+GAMMA*X(2)+DELTA*X(2)
      SOL(NS+1)=BETA*X(NS+1)+GAMMA*X(NS)+DELTA*X(NS)
      DO 56 I=2,NS
   56 SOL(I)=BETA*X(I)+GAMMA*X(I-1)+DELTA*X(I+1)
   87 PUNCH 89
      TYPE 89
   89 FORMAT(//19X,23HSMOOTHED POWER SPECTRUM)
      PUNCH 90,(SOL(I),I=1,J1)
      TYPE 90, (SOL(I),I=1,J1)
   90 FORMAT(5(2X,F14.7))
      TYPE 208
  208 FORMAT(44HSMOOTHED POWER SPECTRUM COMPUTED-PRESS START)
      PAUSE
      TYPE 108
  108 FORMAT(25HENTER NEW PARAMETERS,DATA)
      PAUSE
      GO TO 100
      END
```

REFERENCES

Bendat, J. S. (1958). Principles and Applications of Random Noise Theory, John Wiley & Sons, Inc., New York, pp. 1-9.

Bhartendu (1964). Acoustics of thunder, Ph. D. Thesis, University of Saskatchewan, Saskatoon, Canada, pp. 76-81.

Blackman, R. B. and J. W. Tukey (1958). The Measurement of Power Spectra, Dover Publications, Inc., New York.

Cramer, H. (1946). Mathematical Methods of Statistics, Princeton University Press, pp. 48-62.

Davenport, W. B., Jr., and W. L. Root (1958). Random Signals and Noise, McGraw-Hill Book Company, Inc., New York, pp. 1-111.

Frantti, G. E., D. E. Willis, and J. J. Wilson (1962). The spectrum of seismic noise, Bull. Seism. Soc. Amer., V. 52, pp. 113-121.

Khinchine, A. I. (1949). Statistical Mechanics, Dover Publications, Inc., New York.

Long, L. T. (1964). A study of short-period microseisms, Masters Thesis, New Mexico Institute of Mining and Technology.

Paulson, K. V. (1964). The analysis of time sequences with reference to geophysical applications, Report No. RS-12, University of Saskatchewan, Institute of Upper Atmospheric Physics.

Sears, F. W. and M. W. Zemansky (1955). University Physics, Addison-Wesley Publishing Company, Inc., Reading, Massachusetts, pp. 394-397.

Shannon, C. E. (1949). Communication in the Presence of Noise, Proceedings of the I. R. E., V. 37, No. 1, pp. 10-21.

Solodovnikov, V. V. (1960). Introduction to the Statistical Dynamics of Automatic Control Systems, Dover Publications, Inc., New York, pp. 63-122.

Walker, R. A., J. Z. Menard, and B. P. Bogert (1964). Real-time, high resolution spectroscopy of seismic background noise, Bull. Seism. Soc. Amer., V. 54, No. 2, pp. 501-509.

This thesis is accepted on behalf of the faculty of the Institute by the following committee:

Allan R. Sanford

Charles Holmes

Ross Lomanitz

Chairman

Date: Jan. 27, 1966